

Influence of a dynamical gluon mass in the pp and $\bar{p}p$ forward scatteringE. G. S. Luna,^{1,2} A. F. Martini,² M. J. Menon,² A. Mihara,³ and A. A. Natale¹¹*Instituto de Física Teórica, Universidade Estadual Paulista, 01405-900, São Paulo, SP, Brazil*²*Instituto de Física Gleb Wataghin, Universidade Estadual de Campinas, 13083-970, Campinas, SP, Brazil*³*Instituto de Física de São Carlos, Universidade de São Paulo, 13560-970, São Carlos, SP, Brazil*

(Received 7 July 2005; published 23 August 2005)

We compute the tree level cross section for gluon-gluon elastic scattering taking into account a dynamical gluon mass, and show that this mass scale is a natural regulator for this subprocess cross section. Using an eikonal approach in order to examine the relationship between this gluon-gluon scattering and the elastic pp and $\bar{p}p$ channels, we found that the dynamical gluon mass is of the same order of magnitude as the *ad hoc* infrared mass scale m_0 underlying eikonalized QCD-inspired models. We argue that this correspondence is not an accidental result, and that this dynamical scale indeed represents the onset of nonperturbative contributions to the elastic hadron-hadron scattering. We apply the eikonal model with a dynamical infrared mass scale to obtain predictions for $\sigma_{tot}^{pp,\bar{p}p}$, $\rho^{pp,\bar{p}p}$, slope $B^{pp,\bar{p}p}$, and differential elastic scattering cross section $d\sigma^{\bar{p}p}/dt$ at Tevatron and CERN-LHC energies.

DOI: [10.1103/PhysRevD.72.034019](https://doi.org/10.1103/PhysRevD.72.034019)

PACS numbers: 12.38.Lg, 13.85.Dz, 13.85.Lg

I. INTRODUCTION

The increase of hadron-hadron total cross sections was theoretically predicted many years ago [1] and this prediction has been accurately verified by experiment [2]. At present the main theoretical approaches to explain this behavior are the Regge pole model and the QCD-inspired models.

In the Regge pole model the increase of the total cross section is attributed to the exchange of a colorless state having the quantum numbers of the vacuum: the Pomeron [3]. In the QCD framework the Pomeron can be understood as the exchange of at least two gluons in a color singlet state [4]. A simple and interesting model for the Pomeron has been put forward where it is evidenced the importance of the QCD nonperturbative vacuum [5]. One of the aspects of this nonperturbative physics appears in an infrared (IR) gluon mass scale which regulates the divergent behavior of the Pomeron exchange.

In the QCD-inspired (or “mini-jet”) models the increase of the total cross sections is associated with semihard scatterings of partons in the hadrons. The energy dependence of the cross sections is driven especially by gluon-gluon scattering processes, where the behavior of the gluon distribution function at small x exhibits the power law $g(x, Q^2) \sim x^{-J}$ (see [6–8] and references therein). In this case it is the gluon-gluon subprocess cross section that is potentially divergent at small transferred momenta. The procedure to regulate this behavior is the introduction of a purely *ad hoc* mass scale which separates the perturbative from the nonperturbative QCD region [9,10]. This mass scale, as well as the fixed coupling constant present in the elementary cross sections, are adjusted in order to obtain the best fits to the experimental data.

On the other hand, several recent works have shown that the gluon may develop a dynamical mass (see the review [11] and the earlier work of Ref. [12]). This dynamical

gluon mass was already successfully introduced in the Pomeron model of Landshoff and Nachtmann [13]. Hence it is natural to ask if the arbitrary mass scale that appears in the QCD-inspired models could be explained at a deeper level in terms of the dynamical gluon mass. This relation seems to be a plausible possibility and in this paper we will show that the dynamical gluon mass, as well as the IR finite coupling constant associated to it [14], are in fact the natural regulators for the cross sections calculations. Since the behavior of the running coupling constant is constrained by the value of the dynamical gluon mass [12,14], we will be able to substitute the two *ad hoc* parameters in the “mini-jet” models [6–8], namely, the infrared mass scale (m_0) and the effective value of the running coupling constant (α_s), by a physically well motivated one. In this way, beyond the natural interpretation of the arbitrary infrared mass scale in terms of a dynamical one, it is possible to decrease the number of parameters in this line of models.

The paper is organized as follows: In the next section we introduce a dynamical gluon mass in the gluon-gluon scattering and compare the result to the standard one used in QCD-inspired models. In Sec. III we develop a QCD-inspired eikonal model in the light of the calculation of Sec. II. Our results are presented in the Sec. IV, where the best value for the dynamical gluon mass is determined and used thereafter to determine several quantities of pp and $\bar{p}p$ scattering. In Sec. V we present our conclusions.

II. INFRARED MASS SCALE AND GLUON-GLUON ELASTIC SCATTERING

In recent years there have been discussions in the literature about how to merge in a doubtless way the nonperturbative QCD results with the perturbative expansion. It is worth mentioning that Brodsky has several times called attention about the possibility to build up a skeleton ex-

pansion where the nonperturbative information would be included in vertices and propagators. In particular, the freezing of the QCD running coupling constant at low energy scales could allow to capture at an inclusive level the nonperturbative effects in a reliable way (see, for instance, Ref. [15]). The freezing of the coupling constant and the existence of a dynamical gluon mass are intimately connected [14], therefore they should appear systematically in this sought expansion.

It is possible that such skeleton expansion could appear with the use of the pinch technique [16]. With this technique the nonperturbative behavior of “gauge invariant” propagators and vertices could be computed nonperturbatively at one given order and substituted into the perturbative skeleton expansion. The fact that the “pinch” parts help to form gauge invariant quantities would result in well behaved matrix elements for the desired expansion.

It is clear that we are still far from the kind of expansion discussed above, and we have to rely on more phenomenological approaches to go forward in this direction. One attempt to understand the effect of dynamically massive gluons was performed by Forshaw, Papavassiliou and Parrinello [17], where they do introduce bare massive gluons and study the amplitude behavior for some tree and one-loop level diagrams that could be relevant for diffractive scattering. In this approach, for example, the amplitude for the tree level process $q\bar{q} \rightarrow gg$ comes out with a mass dependence which is washed out in the high-energy limit, but the massless limit is not recovered due to the presence of a numerically small mass independent term. The calculation is instructive but does not reproduce the high-energy limit of massless gluons with 2 degrees of freedom, as discussed by Slavnov many years ago [18]. Actually the dynamical masses go to zero at large momenta and we should expect to recover the elementary cross sections of perturbative QCD in the high-energy limit. Following this thought we could say that the sum over the polarizations should be performed as if the gluons were massless otherwise we would not map (at high energies) the desired skeleton expansion into the perturbative QCD expansion.

According to the above discussion, we cannot work with a massive Yang-Mills theory or use a massive model where the third polarization state is provided by a massless scalar field. Thus, we will just assume a phenomenological procedure stated many years ago by Pagels and Stokar and named dynamical perturbation theory (DPT) [19]. The DPT approximation can be described as follows: amplitudes that do not vanish to all orders of perturbation theory are given by their free-field values. On the other hand, amplitudes that vanish in all orders in perturbation theory as $\propto \exp(-1/g^2)$ (g is the coupling constant) are retained at lowest order. In our case this means that the effects of the dynamical gluon mass in the propagators and vertices will be retained, and the sum of polarizations will be performed

for massless (free-field) gluons, because its signal (for massive gluons) will not vanish from the elementary cross section. In this approach, the differential elastic cross section for the process $gg \rightarrow gg$ is written as

$$\frac{d\hat{\sigma}^{DPT}}{d\hat{t}}(\hat{s}, \hat{t}) = \frac{9\pi\bar{\alpha}_s^2}{2\hat{s}^2} \left[3 - \frac{\hat{s}[4M_g^2 - \hat{s} - \hat{t}]}{[\hat{t} - M_g^2]^2} - \frac{\hat{s}\hat{t}}{[3M_g^2 - \hat{s} - \hat{t}]^2} - \frac{\hat{t}[4M_g^2 - \hat{s} - \hat{t}]}{[\hat{s} - M_g^2]^2} \right], \quad (1)$$

where $\bar{\alpha}_s$ and M_g^2 are the expressions for the nonperturbative running coupling constant and for the dynamical gluon mass, respectively. They were obtained by Cornwall [12] by means of the pinch technique in order to derive a gauge invariant Schwinger-Dyson equation for the gluon propagator. These expressions are given by

$$\bar{\alpha}_s(q^2) = \frac{4\pi}{\beta_0 \ln[(q^2 + 4M_g^2(q^2))/\Lambda^2]}, \quad (2)$$

$$M_g^2(q^2) = m_g^2 \left[\frac{\ln(q^2 + 4m_g^2)}{\ln\frac{\Lambda^2}{\Lambda^2}} \right]^{-12/11}, \quad (3)$$

where $\beta_0 = 11 - \frac{2}{3}n_f$ (n_f is the number of flavors) and Λ ($\equiv \Lambda_{QCD}$) is the QCD scale parameter. The latter expression has been determined as a fit to the numerical solution for the gluonic Schwinger-Dyson equation in the case of pure gauge QCD [12]. We also assume that the introduction of fermions does not change drastically this behavior. The gluon mass scale m_g has to be found phenomenologically, and a typical value is $m_g = 500 \pm 200$ MeV (for $\Lambda = 300$ MeV) [12,20]. Note that we present the full $gg \rightarrow gg$ cross section just for completeness, where the terms suppressed by powers of \hat{s} are not important compared to leading $\ln\hat{s}$ perturbative corrections. However it should be pointed out that up to now higher order corrections have not been introduced in these type of models, and this is even more complicated if we consider the nonperturbative effects that we are introducing in this work.

A different expression for the dynamical gluon mass can be found in Ref. [21], given by

$$M_g^2(q^2) = \frac{m_g^4}{q^2 + m_g^2}, \quad (4)$$

which is consistent with the asymptotic behavior of $M_g(q^2)$ in the presence of the gluon condensates [22]. However, the calculation of the hadronic cross section does not depend strongly on the specific form of $M_g(q^2)$, but more on its IR value (i.e., the value of m_g).

In the limit $q^2 \gg \Lambda^2$, the dynamical mass $M_g(q^2)$ vanishes, and the nonperturbative QCD running coupling $\bar{\alpha}_s$ matches with the one-loop perturbative QCD one. Thus, in

the limit of large enough q^2 , the expression (1) reproduces its perturbative QCD counterpart:

$$\frac{d\hat{\sigma}^{QCD}}{d\hat{t}}(\hat{s}, \hat{t}) = \frac{9\pi\alpha_s^2}{2\hat{s}^2} \left[3 + \frac{\hat{s}(\hat{s} + \hat{t})}{\hat{t}^2} - \frac{\hat{s}\hat{t}}{(\hat{s} + \hat{t})^2} + \frac{\hat{t}(\hat{s} + \hat{t})}{\hat{s}^2} \right]. \quad (5)$$

To compute (1) we have used a vertex having a momentum dependent running coupling and a massive gluon propagator in the Feynman gauge, where the sum over gluon polarizations was performed for massless gluons.

The total cross section $\hat{\sigma}(\hat{s}) = \int_{\hat{t}_{\min}}^{\hat{t}_{\max}} (d\hat{\sigma}/d\hat{t}) d\hat{t}$ for the subprocess $gg \rightarrow gg$, that will be used in the next section to compose the eikonal term χ_{gg} , is obtained by integrating over $4m_g^2 - \hat{s} \leq \hat{t} \leq 0$. In setting these kinematical limits we have neglected the momentum behavior in Eq. (3), as expected from our discussion on the weak dependence of hadronic cross sections on the specific form of $M_g^2(q^2)$. A straightforward calculation yields

$$\begin{aligned} \hat{\sigma}^{DPT}(\hat{s}) &= \frac{3\pi\bar{\alpha}_s^2}{\hat{s}} \\ &\times \left[\frac{12\hat{s}^4 - 55m_g^2\hat{s}^3 + 12m_g^4\hat{s}^2 + 66m_g^6\hat{s} - 8m_g^8}{4m_g^2\hat{s}[\hat{s} - m_g^2]^2} \right. \\ &\left. - 3\ln\left(\frac{\hat{s} - 3m_g^2}{m_g^2}\right) \right]. \quad (6) \end{aligned}$$

The asymptotic energy (\hat{s}) dependence of the total cross section $\hat{\sigma}^{DPT}(\hat{s})$ is of the following form

$$\hat{\sigma}^{DPT}(\hat{s}) \approx \frac{9\pi\bar{\alpha}_s^2}{m_g^2}. \quad (7)$$

We notice that the above result is similar to the asymptotic expression for the gluon-gluon total elastic cross section usually adopted in QCD-inspired models (QIM),

$$\hat{\sigma}^{QIM}(\hat{s}) \equiv \Sigma_{gg} = \frac{9\pi\alpha_s^2}{m_0^2}, \quad (8)$$

where the parameters m_0 and α_s are assumed to be equal to 0.6 GeV and 0.5, respectively [7,8]. We particularly call attention to these values, because they are of the same order of magnitude as the dynamical gluon mass scale (m_g) and its frozen IR value of the coupling constant, obtained in other calculations of strongly interacting processes [20]. Therefore, all the point in here is how to connect these nonperturbative results to the straightforward perturbative QCD calculations.

III. DYNAMICAL GLUON MASS AND QCD-INSPIRED EIKONAL MODELS

A consistent calculation of high-energy hadron-hadron cross sections must be compatible with analyticity and unitarity constraints. The latter can be automatically satisfied by use of an eikonalized treatment of the semihard

parton processes. In an eikonal representation, the total, elastic and inelastic cross sections are given by

$$\sigma_{tot}(s) = 4\pi \int_0^\infty b db [1 - e^{-\chi_I(b,s)} \cos \chi_R(b,s)], \quad (9)$$

$$\sigma_{el}(s) = 2\pi \int_0^\infty b db |1 - e^{-\chi_I(b,s) + i\chi_R(b,s)}|^2, \quad (10)$$

$$\sigma_{in}(s) = \sigma_{tot}(s) - \sigma_{el}(s) = 2\pi \int_0^\infty b db [1 - e^{-2\chi_I(b,s)}], \quad (11)$$

respectively, where s is the square of the total center-of-mass energy and $\chi(b,s)$ is a complex eikonal function: $\chi(b,s) = \chi_R(b,s) + i\chi_I(b,s)$. In this formalism, the factor $e^{-2\chi_I(b,s)}$ in the expression (11) is interpreted as the probability that neither nucleon is broken up in a collision at impact parameter b . The ratio ρ of the real to the imaginary part of the forward scattering amplitude is given by

$$\rho(s) = \frac{\text{Re}\{i \int b db [1 - e^{i\chi(b,s)}]\}}{\text{Im}\{i \int b db [1 - e^{i\chi(b,s)}]\}}, \quad (12)$$

whereas the nuclear slope B and the differential elastic scattering cross section are given by

$$B(s) = \frac{\int b^3 db [1 - e^{i\chi(b,s)}]}{\int b db [1 - e^{i\chi(b,s)}]}, \quad (13)$$

and

$$\frac{d\sigma_{el}}{dt}(s, t) = \frac{1}{2\pi} \left| \int b db [1 - e^{i\chi(b,s)}] J_0(qb) \right|^2, \quad (14)$$

respectively, where $J_0(x)$ is the Bessel function of the first kind. The eikonal function can be written as a combination of an even and odd eikonal terms related by crossing symmetry. In terms of the proton-proton (pp) and antiproton-proton ($\bar{p}p$) scatterings, this combination reads $\chi_{pp}^{\bar{p}p}(b,s) = \chi^+(b,s) \pm \chi^-(b,s)$.

Following the work of Block *et al.* [8], we write the even eikonal as the sum of gluon-gluon, quark-gluon, and quark-quark contributions:

$$\begin{aligned} \chi^+(b,s) &= \chi_{qq}(b,s) + \chi_{qg}(b,s) + \chi_{gg}(b,s) \\ &= i[\sigma_{qq}(s)W(b; \mu_{qq}) + \sigma_{qg}(s)W(b; \mu_{qg}) \\ &\quad + \sigma_{gg}(s)W(b; \mu_{gg})]. \quad (15) \end{aligned}$$

Here $W(b; \mu)$ is the overlap function at impact parameter space and $\sigma_{ij}(s)$ is the elementary subprocess cross section of colliding quarks and gluons ($i, j = q, g$). The overlap function is usually associated with the Fourier transform of a dipole form factor,

$$W(b; \mu) = \frac{\mu^2}{96\pi} (\mu b)^3 K_3(\mu b), \quad (16)$$

where $K_3(x)$ is the modified Bessel function of second kind. The $W(b; \mu)$ function is normalized so that $\int d^2\vec{b}W(b; \mu) = 1$. The odd eikonal $\chi^-(b, s)$, that accounts for the difference between pp and $\bar{p}p$ channels, is parametrized as

$$\chi^-(b, s) = C_{\text{odd}} \Sigma_{gg} \frac{m_0}{\sqrt{s}} e^{i\pi/4} W(b; \mu_{\text{odd}}), \quad (17)$$

where Σ_{gg} is given by the expression (8) and m_0 is an arbitrary IR mass scale. C_{odd} and μ_{odd} are fitting parameters. We borrow this term, with its correct analyticity property, and write our odd eikonal as

$$\chi^-(b, s) = C^- \Sigma \frac{m_g}{\sqrt{s}} e^{i\pi/4} W(b; \mu^-), \quad (18)$$

where m_g is the dynamical gluon mass and the parameters C^- and μ^- are constants to be fitted. The factor Σ is defined as

$$\Sigma = \frac{9\pi\bar{\alpha}_s^2(0)}{m_g^2}, \quad (19)$$

which is just the expression (7) deprived of any momentum dependence, with the coupling constant $\bar{\alpha}_s$ set at its frozen IR value. This definition of Σ , when compared with the Σ_{gg} one, reveals explicitly the natural relation between the infrared mass scales m_0 and m_g .

In the original Block *et al.* model the eikonal functions $\chi_{qq}(b, s)$ and $\chi_{qg}(b, s)$, needed to describe the lower-energy forward data, are parametrized with terms dictated by the Regge phenomenology. Similarly, we parametrize our quark-quark and quark-gluon contributions as

$$\chi_{qq}(b, s) = i\Sigma A \frac{m_g}{\sqrt{s}} W(b; \mu_{qq}), \quad (20)$$

$$\chi_{qg}(b, s) = i\Sigma \left[A' + B' \ln\left(\frac{s}{m_g^2}\right) \right] W(b; \sqrt{\mu_{qq}\mu_{gg}}), \quad (21)$$

where A, A', B', μ_{qq} and μ_{gg} are fitting parameters. Notice that in the above expression the inverse size (in impact parameter) μ_{qg} is defined in the same way as in the original model, i.e., $\mu_{qg} \equiv \sqrt{\mu_{qq}\mu_{gg}}$. In deriving the expressions (20) and (21) we have used the fact that the main contribution to the asymptotic behavior of hadron-hadron total cross sections comes from gluon-gluon semihard collisions, since $g(x) \gg q(x)$ at small- x values. Therefore it is enough to build instrumental quark-quark and quark-gluon parametrizations for the expected high-energy behavior of the pp and $\bar{p}p$ amplitudes and to compute only the gluon-gluon contribution by means of the calculation procedure described in the last section. For example, the term $\ln(s/m_g^2)$ is naturally explained by the presence of a massive gluon in the $qg \rightarrow qg$ subprocess. In this way the chosen eikonals reflect exactly the terms that come from such cross section calculations. We also have not consid-

ered the effect of dynamically generated quark masses in the subprocesses involving quarks. This approach involves an extra parameter ($m_q \approx 250 - 300$ MeV), but we believe that its effect is smaller compared to the dynamical gluon mass one.

The gluon-gluon contribution dominates at high energy and determines the asymptotic behavior of the total cross section. In our model we associate the gluon eikonal term $\chi_{gg}(b, s)$ (see the expression (15)) with the cross section $\sigma_{gg}^{DPT}(s)$: $\chi_{gg}(b, s) \equiv \sigma_{gg}^{DPT}(s)W(b; \mu_{gg})$. Hence the gluon eikonal contribution includes $gg \rightarrow gg$ subprocesses with color nonsinglet exchange in all possible channels. The cross section $\sigma_{gg}^{DPT}(s)$ is written as

$$\sigma_{gg}^{DPT}(s) = C' \int_{4m_g^2/s}^1 d\tau F_{gg}(\tau) \hat{\sigma}^{DPT}(\hat{s}), \quad (22)$$

where $F_{gg}(\tau)$ is the convoluted structure function for pair gg , $\hat{\sigma}^{DPT}(\hat{s})$ is the subprocess cross section given by expression (6), and C' is a fitting parameter. In the above expression we have introduced the energy threshold $\hat{s} \geq 4m_g^2$ for the final state gluons, assuming that these are screened gluons, in a procedure similar to the calculation of Ref. [23]. The structure function $F_{gg}(\tau)$ is written as

$$F_{gg}(\tau) = [g \otimes g](\tau) = \int_{\tau}^1 \frac{dx}{x} g(x) g\left(\frac{\tau}{x}\right), \quad (23)$$

where $g(x)$ is the gluon distribution function, usually adopted as

$$g(x) = N_g \frac{(1-x)^5}{x^J}, \quad (24)$$

where $J = 1 + \epsilon$ and $N_g = \frac{1}{240}(6 - \epsilon)(5 - \epsilon)\dots(1 - \epsilon)$. In this definition the term $\sim 1/x^{1+\epsilon}$ simulates the effect of scaling violations in the small x behavior of $g(x)$ [10]. In the Regge language the quantity J , that controls the asymptotic behavior of $\sigma_{tot}(s)$, is the so called intercept of the Pomeron. In fact, neglecting the variation with q^2 of the asymptotic expression (7), it is possible to show that

$$\lim_{\hat{s} \rightarrow \infty} \int_{4m_g^2/s}^1 d\tau F_{gg}(\tau) \hat{\sigma}^{DPT}(\hat{s}) \sim \left(\frac{s}{4m_g^2}\right)^\epsilon. \quad (25)$$

Hence the total cross section behaves asymptotically as a Pomeron power law s^{J-1} , and a consistent value of J can be determined by fitting forward quantities data through a Regge pole model. Recently, by means of an extended Regge model, some authors have determined the bounds for the soft Pomeron intercept imposed by the accelerator and cosmic ray data currently available [24,25]. These results are consistent with a Pomeron intercept $J = 1.085$ (specifically, $J - 1 = 0.085 \pm 0.006$ in the case of constrained bounds [25]), and corroborate the choice of the Pomeron intercept value adopted in this work.

We ensure the correct analyticity properties of our model amplitudes by substituting $s \rightarrow se^{-i\pi/2}$ throughout

Eqs. (20)–(22). For simplicity, we will refer to our QCD-inspired model with a dynamical gluon mass simply as the DGM model.

IV. RESULTS

In all the fits performed in this paper we use a χ^2 fitting procedure, where the value of χ^2_{\min} is distributed as a χ^2 distribution with N degrees of freedom (DOF). The fits to the experimental data sets are performed adopting an interval $\chi^2 - \chi^2_{\min}$ corresponding, in the case of normal errors, to the projection of the χ^2 hypersurface containing 90% of probability. In the case of the DGM model (8 fitting parameters) this corresponds to the interval $\chi^2 - \chi^2_{\min} = 13.36$ [26]. To determine the optimum value for the dynamical gluon mass and extract the best phenomenological values of the DGM model parameters, we follow a two step process. First, we select specific input values for the dynamical gluon mass and carry out global fits to all high-energy forward pp and $\bar{p}p$ scattering data above $\sqrt{s} = 10$ GeV and to the elastic differential scattering cross section for $\bar{p}p$ at $\sqrt{s} = 1.8$ TeV. These forward data sets include the total cross section (σ_{tot}), the ratio of the real to imaginary part of the forward scattering amplitude (ρ), and the nuclear slope in the forward direction (B). We use the data sets compiled and analyzed by the Particle Data Group [2], to which we add the new E811 data on $\sigma_{\text{tot}}^{\bar{p}p}$ and $\rho^{\bar{p}p}$ at $\sqrt{s} = 1.8$ TeV [27]. The statistic and systematic errors of the forward quantities have been added in quadrature. The input values of the m_g have been chosen to lie in the interval [300 800] MeV, as suggested by the value $m_g = 500 \pm 200$ usually obtained in other calculations of strongly interacting processes (see Sec. II). Although no physical argument ensures that the optimum value of m_g

TABLE I. Values of the parameters of the DGM model resulting from the global fit to the forward pp and $\bar{p}p$ data. The dynamical gluon mass scale was set to $m_g = 400$ MeV.

C'	$(12.097 \pm 0.962) \times 10^{-3}$
μ_{gg} [GeV]	0.7242 ± 0.0172
A	6.72 ± 0.92
μ_{qq} [GeV]	1.0745 ± 0.0405
A'	$(4.491 \pm 0.179) \times 10^{-3}$
B'	1.08 ± 0.14
C^-	3.17 ± 0.35
μ^- [GeV]	0.6092 ± 0.0884

lies in the chosen input mass interval, our global fit results indicate a minimum value just about $m_g \approx 400$ MeV. These results are shown in Fig. 1, where a general dashed curve is added to guide the eye. Roughly, taking a 5% variation on the minimal χ^2/DOF value indicated by the general curve, it is possible to estimate a dynamical gluon mass $m_g \approx 400^{+350}_{-100}$ MeV. This result is totally compatible with the ones of Ref. [13]: $m_g = 370$ MeV.

Next, in order to determine the parameters of the DGM model, we set the value of the dynamical gluon mass to $m_g = 400$ MeV (optimal value) and carry out a global fit only to all high-energy forward pp and $\bar{p}p$ scattering data above $\sqrt{s} = 10$ GeV, not including the elastic differential scattering cross section $d\sigma^{\bar{p}p}/dt$ at $\sqrt{s} = 1.8$ TeV. The values of the fitted parameters are given in Table I. The χ^2/DOF for this global fit was 1.075 for 188 degrees of freedom. The results of the fits to σ_{tot} , ρ and B for both pp and $\bar{p}p$ channels are displayed in Figs. 2–4, , respectively, together with the experimental data. Within this procedure, the Tevatron differential cross section, as well as the Tevatron-run II and the CERN LHC ones, can be predicted

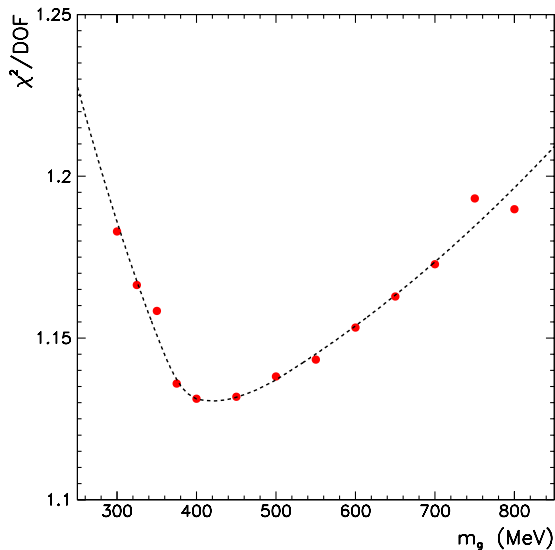


FIG. 1 (color online). The χ^2/DOF as a function of dynamical gluon mass m_g .

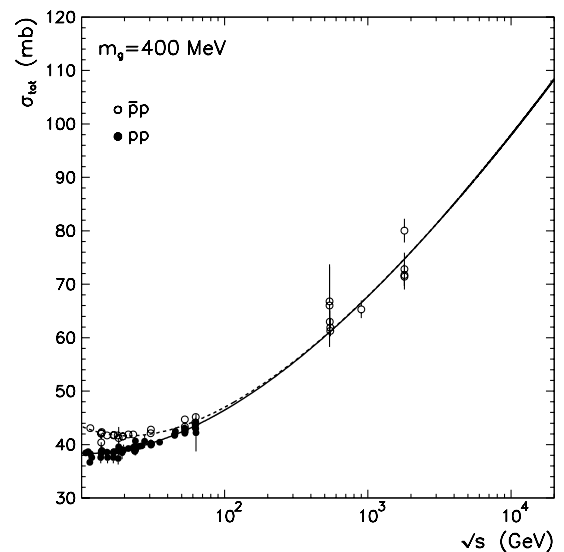


FIG. 2. Total cross section for pp (solid curve) and $\bar{p}p$ (dashed curve) scattering.

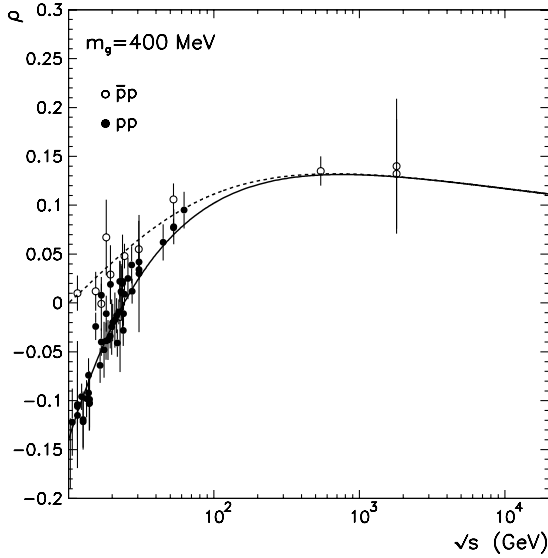


FIG. 3. Ratio of the real to imaginary part of the forward scattering amplitude for pp (solid curve) and $\bar{p}p$ (dashed curve) scattering.

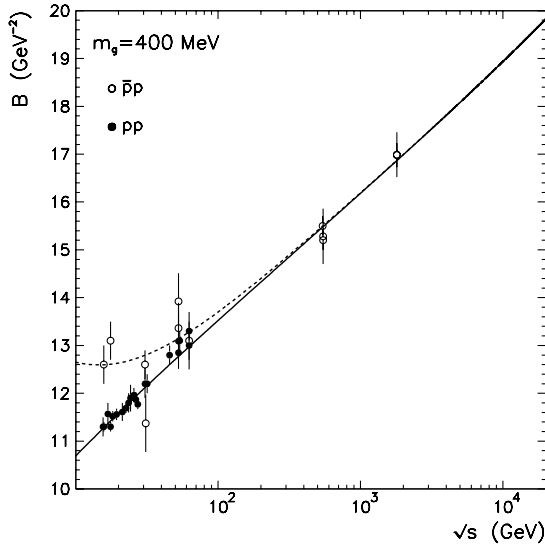


FIG. 4. Nuclear slope parameter for elastic pp (solid curve) and $\bar{p}p$ (dashed curve) scattering.

by the DGM model. These predictions are shown in Fig. 5. Table II contains predictions for the forward quantities at these energies, where the quoted errors are the statistical errors due to the errors in the fitted parameters.

TABLE II. Predictions of the pp and $\bar{p}p$ forward scattering quantities σ_{tot} , ρ and B for the Fermilab Tevatron run-II (TEVII) and the CERN LHC energies.

	TEVII [1.96 TeV]	LHC [14 TeV]
$\sigma_{tot}^{pp}, \sigma_{tot}^{\bar{p}p}$ [mb]	75.7 ± 5.4	102.9 ± 7.1
$\rho^{pp}, \rho^{\bar{p}p}$	0.129 ± 0.009	0.114 ± 0.005
$B^{pp}, B^{\bar{p}p}$ [GeV^{-2}]	16.97 ± 0.99	19.36 ± 1.12

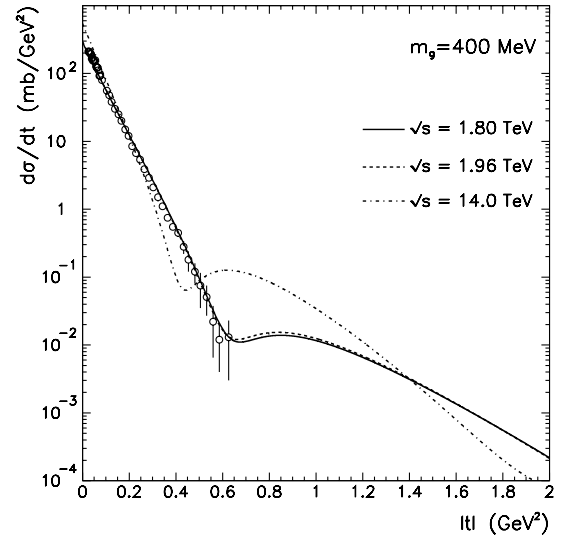


FIG. 5. Predictions for the elastic differential scattering cross sections at $\sqrt{s} = 1.8, 1.96$ and 14 TeV. In our model the channels pp and $\bar{p}p$ are not distinguished at high energies. The data points are from E710 [28].

V. CONCLUSIONS

In this paper we have investigated the influence of an infrared dynamical gluon mass scale in the calculation of pp and $\bar{p}p$ forward scattering quantities through a QCD-inspired eikonal model. By means of the dynamical perturbation theory (DPT), we have computed the tree level $gg \rightarrow gg$ cross section taking into account the dynamical gluon mass, and have shown that the IR divergences associated with the gluon-gluon subprocess cross section are naturally regulated by this dynamical scale. In order to make a connection between the total subprocess cross section $\hat{\sigma}_{gg}(\hat{s})$ and the forward pp and $\bar{p}p$ quantities, we have developed a QCD-inspired eikonal model where the onset of the dominance of gluons in the interaction of high-energy hadrons is managed by the dynamical gluon mass scale. Using this formalism it was possible not only to reduce the number of parameters of the model, but also to give a consistent physical explanation for each one. For example, in some recent papers on QCD-inspired models [7,8], the two arbitrary constants m_0 and α_s were assumed to be equal 0.6 GeV and 0.5 , respectively; in our approach the IR value of running coupling constant is driven by the dynamical gluon mass, i.e., its IR behavior depends on the value of m_g . This connection permit us to decrease the number of parameters required to describe the hadronic experimental data.

By means of a global fit to the forward pp and $\bar{p}p$ scattering data and to $d\sigma^{\bar{p}p}/dt$ data at $\sqrt{s} = 1.8$ TeV, we have determined the best phenomenological value of the dynamical gluon mass, namely $m_g \approx 400^{+350}_{-100}$ MeV. Interestingly enough, this value is of the same order of magnitude as the value $m_g \approx 500 \pm 200$ MeV, obtained in

other calculations of strongly interacting processes. This result corroborates theoretical analysis taking into account the possibility of dynamical mass generation and show that, in principle, a dynamical nonperturbative gluon propagator may be used in calculations as if it were a usual (derived from Feynman rules) gluon propagator.

With the dynamical gluon mass set at $m_g = 400$ MeV, we have performed a global fit only to the forward pp and $\bar{p}p$ scattering data, in the same way as is usually performed in the former QCD-inspired models. Our model allows us to describe successfully the forward scattering quantities σ_{tot} , ρ and B , as well as to predict the $\bar{p}p$ differential cross section at $\sqrt{s} = 1.8$ TeV in excellent agreement with the available experimental data. These results show that the DGM model is well suited for detailed predictions of the forward quantities to be measured at higher energies. In particular, for the total cross sections to be measured at Tevatron-run II and CERN-LHC energies, the model predicts the values $\sigma_{tot} = 75.7 \pm 5.4$ mb and $\sigma_{tot} = 102.9 \pm 7.1$ mb, respectively. Our central LHC value prediction is close to the central one in the

Ref. [8], namely $\sigma_{tot} = 108$ mb. This relatively small difference reflects the fact that the dynamical gluon mass and its associated coupling constant successfully replace the values of the *ad hoc* parameters of the former QCD-inspired models. However, if the pp total cross section is measured at the LHC with a precision up to 5%, a selection between these QCD models may be possible.

In summary, we argue that the QCD-inspired eikonal model with a dynamical IR mass scale provides an useful phenomenological tool to the study of the hadron-hadron diffractive scattering, where a purely perturbative QCD method is inadequate.

ACKNOWLEDGMENTS

This research was supported by the Conselho Nacional de Desenvolvimento Científico e Tecnológico-CNPq under contract 151360/2004-9 (EGSL, AAN), and by the Fundação de Amparo à Pesquisa do Estado de São Paulo-FAPESP under constructs 2004/10619-9 (MJM) and 2003/00928-1 (AM).

-
- [1] H. Cheng and T. T. Wu, Phys. Rev. Lett. **24**, 1456 (1970); C. Bourrely, J. Soffer, and T. T. Wu, Phys. Rev. Lett. **54**, 757 (1985); H. Cheng and T. T. Wu, *Expanding Protons: Scattering at High Energies* (MIT Press, Cambridge, MA, 1987).
 - [2] K. Hagiwara *et al.*, Phys. Rev. D **66**, 010001 (2002).
 - [3] P. D. B. Collins, *Regge Theory and High Energy Physics* (Cambridge University Press, Cambridge, 1977); S. Donnachie, G. Dosh, P. Landshoff, and O. Nachtmann, *Pomeron Physics and QCD* (Cambridge University Press, Cambridge, 2002); V. Barone and E. Predazzi, *High-Energy Particle Diffraction* (Springer-Verlag, Berlin, 2002).
 - [4] F. E. Low, Phys. Rev. D **12**, 163 (1975); S. Nussinov, Phys. Rev. Lett. **34**, 1286 (1975).
 - [5] P. V. Landshoff and O. Nachtmann, Z. Phys. C **35**, 405 (1987).
 - [6] M. M. Block *et al.*, Nucl. Phys. B Proc. Suppl. **12**, 238 (1990).
 - [7] M. M. Block, F. Halzen, and B. Margolis, Phys. Rev. D **45**, 839 (1992).
 - [8] M. M. Block, E. M. Gregores, F. Halzen, and G. Pancheri, Phys. Rev. D **60**, 054024 (1999).
 - [9] P. L'Heureux and B. Margolis, Phys. Rev. D **28**, 242 (1983).
 - [10] B. Margolis *et al.*, Phys. Lett. B **213**, 221 (1988).
 - [11] R. Alkofer and L. von Smekal, Phys. Rep. **353**, 281 (2001).
 - [12] J. M. Cornwall, Phys. Rev. D **26**, 1453 (1982); J. M. Cornwall and J. Papavassiliou, Phys. Rev. D **40**, 3474 (1989); J. Papavassiliou and J. M. Cornwall Phys. Rev. D **44**, 1285 (1991).
 - [13] M. B. Gay Ducati, F. Halzen, and A. A. Natale, Phys. Rev. D **48**, 2324 (1993); F. Halzen, G. Krein, and A. A. Natale, Phys. Rev. D **47**, 295 (1993).
 - [14] A. C. Aguilar, A. A. Natale, and P. S. Rodrigues da Silva, Phys. Rev. Lett. **90**, 152001 (2003).
 - [15] S. J. Brodsky, hep-ph/0111127; Acta Phys. Pol. B **32**, 4013 (2001); Fortschr. Phys. **50**, 503 (2002).
 - [16] D. Binosi and J. Papavassiliou, Phys. Rev. D **66**, 111901 (2002); J. Phys. G **30**, 203 (2004).
 - [17] J. R. Forshaw, J. Papavassiliou, and C. Parrinello, Phys. Rev. D **59**, 074008 (1999).
 - [18] A. A. Slavnov, Theor. Math. Phys. (Engl. Transl.) **10**, 201 (1972).
 - [19] H. Pagels and S. Stokar, Phys. Rev. D **20**, 2947 (1979).
 - [20] A. C. Aguilar, A. Mihara, and A. A. Natale, Phys. Rev. D **65**, 054011 (2002); Int. J. Mod. Phys. A **19**, 249 (2004).
 - [21] A. C. Aguilar and A. A. Natale, J. High Energy Phys. **08** (2004) 057.
 - [22] A. C. Aguilar and A. A. Natale, hep-ph/0405024.
 - [23] J. M. Cornwall and A. Soni, Phys. Lett. B **120**, 431 (1983).
 - [24] E. G. S. Luna and M. J. Menon, Phys. Lett. B **565**, 123 (2003).
 - [25] E. G. S. Luna, M. J. Menon, and J. Montanha, Nucl. Phys. A **745**, 104 (2004).
 - [26] W. H. Press *et al.*, *Numerical Recipes: The Art of Scientific Computing* (Cambridge University Press, Cambridge, 1992).
 - [27] C. Avila *et al.*, Phys. Lett. B **537**, 41 (2002).
 - [28] N. Amos *et al.*, Phys. Rev. Lett. **61**, 525 (1988).